SYNTHETIC APERTURE RADAR OBSERVATIONS OF INTERTIDAL FLATS ON THE GERMAN NORTH SEA COAST

Martin Gade [(1)], Sabrina Melchionna [(1)], Kerstin Stelzer [(2)]

[(1)] Universität Hamburg, Institut für Meereskunde, Bundesstr. 53, 20146 Hamburg, Germany,
Email: martin.gade@uni-hamburg.de
[(2)] Brockmann Consult, Max-Planck-Str. 2, 21502 Geesthacht, Germany,
Email: kerstin.stelzer@brockmann-consult.de

ABSTRACT

High-resolution Synthetic Aperture Radar (SAR) data of dry-fallen intertidal flats have been analyzed with respect to the imaging of sediments, macrophytes, and mussels in the German Wadden Sea. A great number of TerraSAR-X and Radarsat-2 images of five test areas along the German North Sea coast were acquired in 2012 and 2013 and form the basis for the present investigation. Depending on the type of sediment, but also on the water level and on environmental conditions (wind speed) exposed sediments may show up on SAR imagery as areas of enhanced radar backscattering. The (multi-temporal) analysis of series of such images allows for the detection of mussel beds, and our results show evidence that also single-acquisition, multi-polarization SAR imagery can be used for that purpose.

1. INTRODUCTION

Intertidal flats are coastal areas that fall dry once during each tidal cycle. Large intertidal flats can be found on the Dutch, German, and Danish North Sea coasts, as well as at other places worldwide, e.g. in South Korea and the United Kingdom. Adopting the Dutch name those areas are often referred to as Wadden areas. The German Wadden Sea is a UNESCO World Natural Heritage, and according to national and international laws a frequent surveillance of the entire area is mandatory.

Remote sensing techniques are ideally suited for the surveillance of areas that are difficult to access. In this respect, Synthetic Aperture Radar (SAR) sensors, because of their all-weather capabilities and their independence of daylight, may be the first choice; however, the radar imaging of bare soils is rather complex, and the very processes responsible for the backscattering of microwaves from exposed intertidal flats are still subject to research. Within the German national project SAMOWatt ("SAR Monitoring of the Wadden Sea") routinely acquired SAR images of dry-fallen intertidal flats on the German North Sea coast are analysed to gain more insight into those scattering mechanisms and to provide a basis for the inclusion of SAR data into existing classification systems of intertidal flats, which are based on optical data [1].
In this paper we present some of our results obtained through the analysis of a great deal of SAR images showing the German Wadden Sea during low tide. The following section introduces the test areas and the data basis, and the next section contains examples of SAR images of exposed intertidal flats and highlights some peculiarities. The section thereafter summarizes some results of the (statistical) image processing results.

2. TEST AREA AND SATELLITE DATA

Five test areas on the German North Sea coast were identified (Fig. 1), which represent areas of typical sediment distributions on intertidal flats, but also include vegetated areas and mussel and oyster beds. Three of them, the test areas "Amrum", "Pellworm" and "Wesselburen" (denoted as "A", "P" and "W", respectively, in Fig. 1) are located in the northern part of the German North Sea coast, in the German National Park "Schleswig-Holstein Wadden Sea". The other two test areas, "Norderney" and "Jadebusen" ("N" and "J", respectively, in Fig. 1), are located further south and are part of the German National Park "Lower Saxonean Wadden Sea".

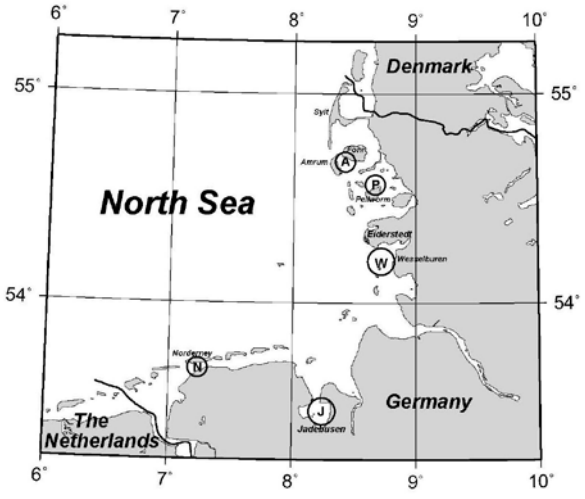

Figure 1. Test areas on the German North Sea coast. A: Amrum; P: Pellworm; W: Wesselburen; N: Norderney; J: Jadebusen

Most of those test areas were already subject to previous studies [2], and they are now complemented by the test

area “Jadebusen”, because of its high spatial heterogeneity and its variability in surface types.

A total of 16 Radarsat-2 and 39 TerraSAR-X SAR images of the SAMOWatt test areas were acquired between June 2012 and June 2013 and form the basis of the analyses presented herein. The Radarsat-2 satellite (hereinafter abbreviated as RS2) was launched in 2007 and carries a C-band SAR working at 5.405 GHz. TerraSAR-X and its sister satellite, TanDEM-X, (hereinafter abbreviated as TSX) were launched in 2007 and 2010, respectively, and they both carry an X-band SAR working at 9.65 GHz. Depending on the acquisition mode, both SAR systems may provide imagery with a pixel size of 1 m, or even below.

3. COMBINED SAR IMAGE ANALYSES

Most of the TSX images were acquired in dual-polarization (Spotlight) mode, thus allowing for a comparison of SAR signatures acquired at vertical (VV) and horizontal (HH) polarizations (the first letter stands for the polarization of the transmitted wave, the second for that of the received wave).

3.1. Multi-polarization analyses

Fig. 2 shows a TSX SAR image of the “Amrum” test area images acquired on June 22, 2013, at 05:41 UTC, 23 minutes after low tide. At the time of image acquisition, a strong wind of 10 m/s from southwest (228°) was reported.

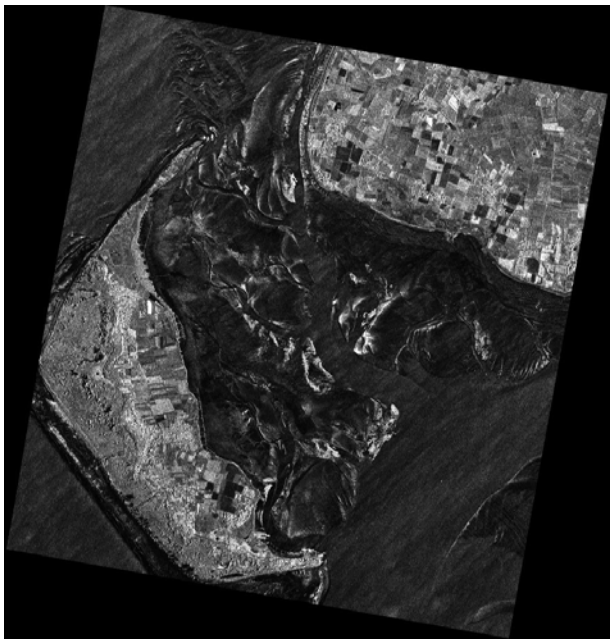

Figure 2. TSX VV-polarization SAR image of the test area “Amrum”, acquired on June 22, 2013, at 05:41 UTC (33 minutes after low tide), © DLR.

Exposed intertidal flats can be identified between the island of Amrum on the left and the island of Föhr on the upper right. Bright areas are often associated with the edges of the tidal channels, thereby pronouncing them on the SAR imagery [3]. However, not all bright patches are due to those channel edges. A number of pronounced, sharp-edged bright patches in the image center are due to oyster beds.

We define the (normalized) polarization coefficient, *PC*, as the ratio of the difference and sum of the two polarization channels, i.e.:

$$PC = \frac{\sigma_{HH} - \sigma_{VV}}{\sigma_{HH} + \sigma_{VV}} \quad (1)$$

where the coefficients σ_{VV} and σ_{HH} are the normalized radar cross sections (NRCS) at vertical and horizontal polarization, respectively. The lower panel in Fig. 3 shows a polarization coefficient map for a (6.3 km × 4.8 km) fragment of the SAR image shown in Fig. 2 (and the respective HH-polarization image). Yellow, orange and red colours denote polarization coefficients well above zero, which corresponds to a (much) stronger backscattering at horizontal polarization. In contrast, blue and purple colours denote negative polarization coefficients, which in turn correspond to (much) stronger backscattering at vertical polarization. Green colours denote neutral coefficients, with radar backscatter values at either polarization of about the same magnitude.

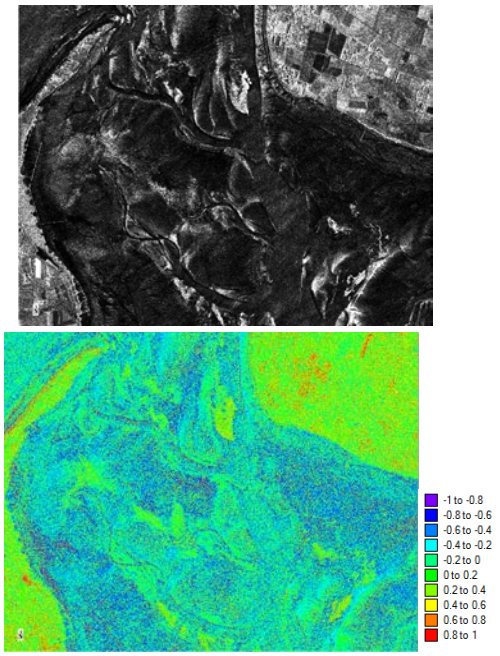

Figure 3. Upper panel: fragment (6.3 km × 4.8 km) of a TSX VV-polarization SAR image of the test area “Amrum” shown in Fig. 2. Lower panel: polarization coefficient calculated from the pair of VV- and HH-polarization TSX SAR images.

Both islands are coloured in green and yellow, since from those areas the radar backscattering at horizontal polarization is as high as, or even higher than, the radar backscattering at vertical polarization. The areas in between the islands are mostly coloured in cyan and blue, because of the higher radar backscattering at vertical polarization. This is in line with radar backscattering theories, which predict stronger vertically polarized radar backscattering from wind-roughened water surfaces and from (moist) bare soils. However, we note that those bright sharp-edged patches seen in the SAR image (upper panel) show up as greenish coloured patches in the polarization coefficient map. Similar to the (dense) vegetation, the oyster beds, because of the heterogeneous orientation of the oyster shells, cause similar backscatter values at both polarization and, thus, green patches in the polarization coefficient maps.

Similar analyses were performed for the test area "Jadebusen" using a TSX SAR image pair acquired on November 14, 2012, at 05:42 UTC, only shortly (7 minutes) after low tide. The VV-polarization image is shown in Fig. 4. At the time of image acquisition, the wind was low (2 m/s) blowing from south (180°). Fig. 5 shows a (5.4 km × 5.0 km) fragment of the full TSX SAR scene in the upper panel and the corresponding polarization coefficient map in the lower panel. Due to the low wind speed the overall backscatter from that area is rather small and, therefore, the SAR image in the upper panel is rather dark. However, there are several bright patches on the SAR image, which are due to extended oyster beds (Fig. 6).

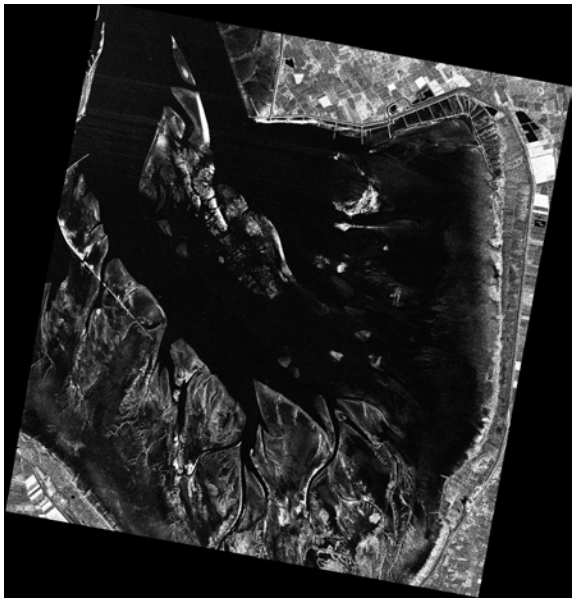

Figure 4. TSX SAR image of the test area "Jadebusen", acquired on November 14, 2012, at 05:42 UTC (7 minutes after low tide), © DLR.

The polarization coefficients calculated from the multi-polarization SAR images (lower panel of Fig. 5) are generally dark, or brownish, i.e., they are a mixture of all colours. That is, the polarization coefficient is changing its sign and magnitude, which is likely to be due to noise effects (which in turn dominate at low wind speeds) and/or to the generally muddy (flat) sediments in that area. Nonetheless, again, the oyster beds can be clearly delineated as greenish patches in the image centre.

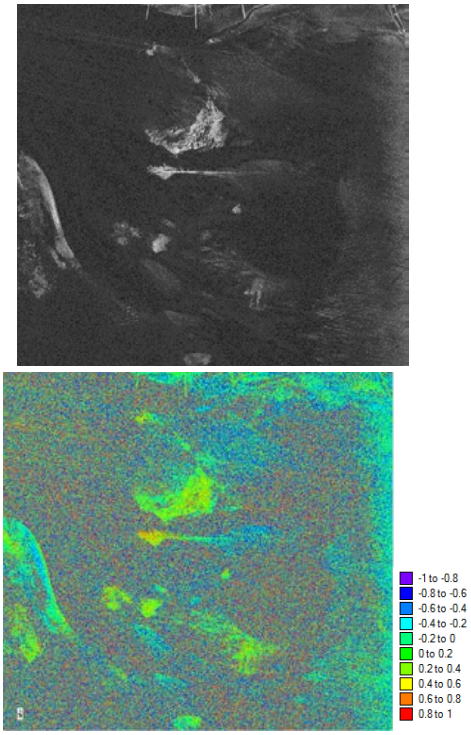

Figure 5. Same as Fig. 3, but for a fragment (5.4 km × 5.0 km) of a TSX SAR image of the test area "Jadebusen", see Fig. 4.

The photograph in Fig. 6 (taken during a field campaign in July 2013 in the test area "Jadebusen", close to the major bright patch in the upper image centre in Fig. 5) shows how the oysters are sticking out of the sediment and how they form "islands" inside the remnant water on the exposed intertidal flats.

Figure 6. Photograph of extended oyster beds in the test area "Jadebusen" (S. Melchionna).

Our results presented herein show that multi-polarization SAR imagery can be used to detect and to classify mussel (oyster) beds on intertidal flats. However, we also note that SAR imagery acquired at steeper incidence angles is less suited for analyses of that kind. The TSX SAR image of November 14, 2012, was acquired at an incidence angle of approx. 40°, but TSX SAR images acquired at steeper incidence angles don't show clear contrasts in the polarization coefficients. This is due to the fact that the difference in radar backscattering at both polarization increases with increasing incidence angle and, therefore, we conclude that the detectability of mussel beds does so as well.

3.2. Multi-temporal analyses

Multi-temporal analyses were performed, which take benefit from the fact that the same spot was imaged (by the same sensor) several times within one vegetation period. We applied basic statistics and calculated the mean and standard deviation for the different radar bands and polarizations. Example results of those multi-temporal analyses using all SAR images of the test area "Pellworm" acquired in 2012 are presented in Fig. 7, where the false colour composites in the upper row and on the bottom left show the mean radar backscatter in green and its standard deviation in magenta. Gade et al. [2] have already shown that these analyses provide valuable information on mussel beds and vegetation on exposed intertidal flats.

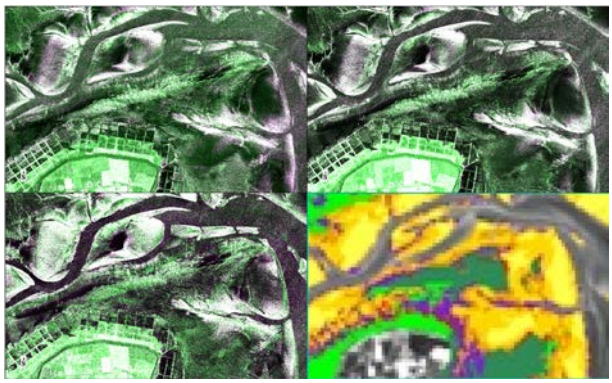

Figure 7. Multi-temporal analyses of TSX and RS2 SAR imagery (2.8 km × 1.6 km) of the "Pellworm" test area. Shown are false color composites of the mean (green) and the standard deviation (magenta) of all SAR images of 2012. Upper left: TSX VV polarization, upper right: TSX HH polarization, lower left: RS2 VV polarization, lower right: classification based on optical imagery © Brockmann Consult.

The upper left panel in Fig. 7 shows those statistical results for all TSX SAR images acquired at VV polarization, the upper right panel for all TSX SAR images acquired at HH polarization, and the lower left panel for all RS2 SAR images acquired at VV polarization (no RS2 HH-polarization images were used). For comparison, a fragment of an existing classification based on optical data [1] is added on the bottom right.

The island of Pellworm always appears green, i.e., the radar backscattering from land is generally high (large mean value, small standard deviation). Many areas on the exposed intertidal flats appear in white, because both the mean value and the standard deviation are large. This is particularly true in the vicinity of the tidal creeks, where the radar backscattering varies most in between the images. The comparison with existing classification data, as those shown in the lower right panel of Fig. 7, reveals that areas, which were classified as vegetated, coincide with those, which generally show a high radar backscatter (whose standard deviation therefore is small and, thus, which are colored green). We therefore note that all radar channels are suitable for the detection of vegetation on dry-fallen intertidal flats, particularly in areas without mussel beds.

4. CONCLUSIONS

We have shown that high-resolution SAR imagery can be used to gain information on the coverage of exposed intertidal flats by vegetation and mussel (oyster) beds. SAR images with pixel sizes of 1 m and below can be used for a detailed surveillance of dry-fallen intertidal flats, especially since those areas are difficult to access.

Multi-polarization SAR imagery can be used to detect oyster beds, if the SAR images were taken at oblique incidence angles (40° in our case), but this capability is reduced at steeper incidence angles. Our results support Choe et al. [4] who recently showed that multi-polarization SAR imagery is suitable for the detection of mussel beds.

However, we also note that a profound knowledge of all main factors contributing to the observed SAR signatures is essential for any improvement of existing classification systems, and our preliminary results show evidence that multi-polarization / multi-satellite SAR data can be used to improve classification systems of intertidal flats.

5. ACKNOWLEGEMENTS

The authors are grateful to the colleagues participating in SAMOWatt, who contributed to the results presented herein. SAMOWatt receives funding from the German Ministry of Economy (BMWi) under contract 50 EE 0817. Radarsat-2 and TerraSAR-X data were provided by CSA and DLR, respectively, under contract 5077/OCE0994.

6. REFERENCES

1. Brockmann, C. & Stelzer K. (2008). Optical Remote

Sensing of Intertidal Flats. In ‘Remote Sensing of the European Seas’ (Eds. V. Barale & M. Gade), Springer, Heidelberg, 514 pp., 117-128.

2. Gade, M., Stelzer, K. & Kohlus, J. (2011). SAR Data Help Improving the Monitoring of Intertidal Flats on the German North Sea Coast. In Proc. 10th Intern. Conf. Mediterr. Coast. Environ., Rhodes, Greece, 25-29 October 2011.

3. Gade, M., Alpers, W., Melsheimer, C. & Tanck, G. (2008). Classification of sediments on exposed tidal flats in the German Bight using multi-frequency radar data. Remote Sens. Environ., 112, 1603-1613, 2008.

4. Choe, B.-H., Kim, D., Hwang, J.-H., Oh, Y. & Moon, W.M. (2012). Detection of oyster habitat in tidal flats using multi-frequency polarimetric SAR data. Estuar. Coast. Shelf Sci. 97, 28-37.